Hot and cold phonons induced by electric field and resonant Raman scattering in GaN/AlN triangular quantum well

Guibao Xu, Suvranta K. Tripathy, Xiaodong Mu, and Yujie J. Ding
Department of Electrical and computer Engineering, Lehigh University, Bethlehem, PA 18015
yud2@Lehigh.edu
Kejia Wang, Cao Yu, and Debdeep Jena
Department of Electrical Engineering, University of Notre Dame, Notre Dame, IN 46556
Jacob B. Khurgin
Department of Electrical and Computer Engineering, Johns Hopkins University, Baltimore, MD 21218

Abstract: We have evidenced hot and cold longitudinal-optical (LO) phonons induced by electric field and resonant Raman scattering in GaN/AlN triangular quantum well, probed by first-order and second-order resonant Raman scattering of 3-ps light pulses.

OCIS codes: (190.5650) Raman effect; (300.6450) Spectroscopy, Raman; (300.6330) Spectroscopy, inelastic scattering including Raman; (190.7220) Upconversion.

The decay time constant for LO phonons in bulk GaN was measured to be a factor of 56 longer than the emission time of the LO phonons by electrons [1]. Due to the accumulation of the LO phonons, phonon temperatures become higher than thermal-equilibrium values. These hot phonons not only cause the electron velocities to saturate but also generate additional heat which needs to be dissipated. Obviously, the performance of the corresponding electronic devices can be sacrificed. Even though phonon temperatures for a biased AlGaN/AlN channel were estimated from noise analysis [2], Raman scattering is one of the most direct techniques for investigating hot phonons.

Here, for the first time, we present our results on the manifestation of the hot LO phonons induced by electric fields in a GaN/AlN triangular quantum well. The first-order and second-order Raman scattering is used to not only determine phonon temperatures but also to study the distributions of the hot phonons in the Brillouin zone. Moreover, we have evidenced the hot and cold LO phonons without the presence of any electric field, which are caused by the first-order Stokes and anti-Stokes Raman scattering of the picosecond light pulses, respectively.

Our GaN/AlN heterostructure consists of a 300-μm sapphire substrate, a 3-μm semi-insulating GaN buffer layer, a 200-nm unintentionally-doped GaN channel layer, and a 4-nm AlN cap layer, which were all grown by MBE except for the substrate in sequence. Due to the polarization and piezoelectric fields at the GaN/AlN interface, high-density two-dimensional electrons were confined in the GaN channel layer by a triangular potential well [3]. Therefore, the electrons drifting in an electric field behave completely different from those in bulk GaN. For all of our measurements, Raman signals propagating in the backward direction were measured for the input wavelength tunable within 369-385 nm, a pulse width of 3 ps, and an average input power of 30 mW.

We measured photoluminescence (PL) spectra pumped by a picosecond coherent UV beam. At each electric field applied parallel to the interface, we deduced the effective bandgap from the corresponding PL spectrum [4], E_g, for the GaN/AlN quantum well and then determined the corresponding lattice temperature by using the Varshni formula [5]. The presence of the high-density electrons causes the effective bandgap to shrink through band-gap renormalization. By tuning the electric field, both the first-order and second-order Raman scattering intensities, determined from Fig. 1(a), are plotted vs. the lattice temperature, see Fig. 1(b). They exhibit resonances at $E_i - E_g \approx 3$ meV [$P_{AS}^{(1)}(0)$] and $E_i - E_g \approx 80$ meV [$P_S^{(1)}(1)$], respectively. For these peaks, free excitons are generated by the incoming photons, which further enhance the Raman signal intensities (i.e. double resonances). Besides these two strong peaks, there are a tail and a shoulder labeled by $P_{AS}^{(1)}(-1)$ and $P_S^{(1)}(0)$ at $E_i - E_g \approx -96$ meV and $E_i - E_g \approx 0$ meV, respectively. These two small features correspond to the resonances of the outgoing and incoming photon energies to the bandgap only, respectively, i.e. single resonances. In our quantum well, the generation of the electrons and their subsequent drift in a dc electric field have further enhanced the resonant peaks of $P_{AS}^{(1)}(0)$ and $P_S^{(1)}(1)$. For these two processes, since the excitons are generated by the incoming photons, they can be quickly ionized to produce electrons and heavy holes. These electrons can gain sufficiently high kinetic energies from the dc electric field and then emit LO phonons. Consequently, the LO phonon occupation number can be significantly increased. The second-order Raman scattering spectra exhibit two resonant peaks, i.e. $P_S^{(2)}(0)$ and $P_{AS}^{(2)}(0)$, at $E_i - E_g(T) \approx 27$ meV and $E_i - E_g(T) \approx 56$ meV, respectively. Without the presence of a dc electric field, we did not observe any second-order anti-Stokes Raman signal regardless of the photon-energy detuning. When the electric field is increased to 4 kV/cm or higher, the second-order anti-Stokes Raman signal becomes visible, see Fig. 1(a).

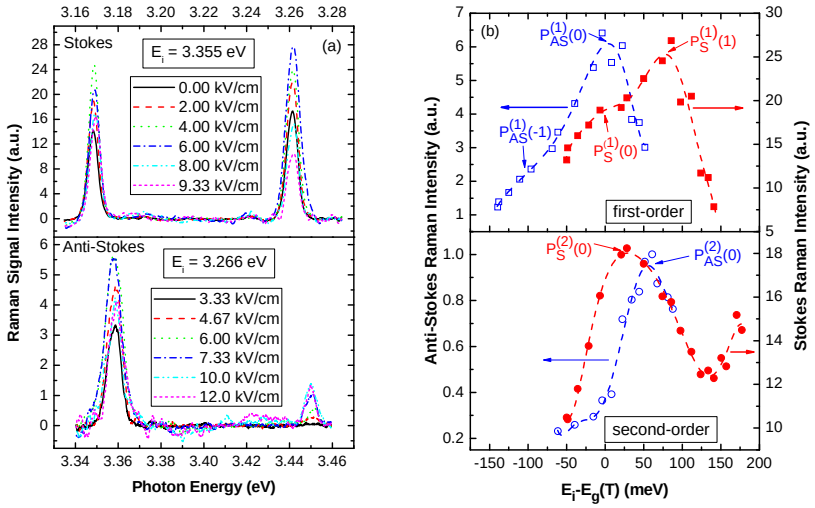

Fig.1. (a) Spectra of first-order (left peaks) and second-order (right peaks) Raman scattering of coherent light pulses by LO phonons with energy of 91.8 meV. (b) Dependences of Raman signal intensities on photon energy of incident beam (E_i), measured relative to bandgap of the GaN/AlN quantum well.

Using the Bose-Einstein distribution function, we have determined the LO-phonon temperatures from the first-order (T_{1LO}) and second order (T_{2LO}) Raman scattering, respectively. For the photon energies of 3.355 eV and 3.266 eV used for the Stokes and anti-Stokes Raman scattering, respectively, T_{1LO} is higher than the lattice temperature by approximately the same amount, i.e. 140 K, within the range of 0-4.67 kV/cm, see Fig. 2(a). However, when the applied electric field exceeds 4.67 kV/cm, T_{1LO} increases much steeper than the lattice temperature. This implies that the additional LO phonons are induced by the applied electric fields. Since T_{2LO} reflects a temperature averaged over the LO phonons within the entire Brillouin zone, it is quite close to the corresponding lattice temperature for the electric fields of 4-6.67 kV/cm. However, T_{2LO} is increased at a higher rate than the lattice temperature. On the other hand, $T_{2LO} < T_{1LO}$ for the entire range of the electric fields, see Fig. 2(a). Moreover, T_{1LO} is increased at a higher rate than T_{2LO} above 6.67 kV/cm. For higher photon energies, T_{1LO} becomes higher at each electric field, including the zero electric field, see Fig. 2(b). Since the additional LO phonons are released by the resonant Stokes Raman scattering of the incident light pulse within 3 ps, the phonon temperature probed by the same light pulse becomes higher (i.e. the *hot* LO phonons even without the presence of any electric field). On the other hand, when the photon energies are lower, the phonon temperatures become lower. This is due to the fact that within 3 ps some of the thermal-equilibrium LO phonons are consumed by resonant anti-Stokes Raman scattering of each incident light pulse (i.e. the *cold* LO phonons).

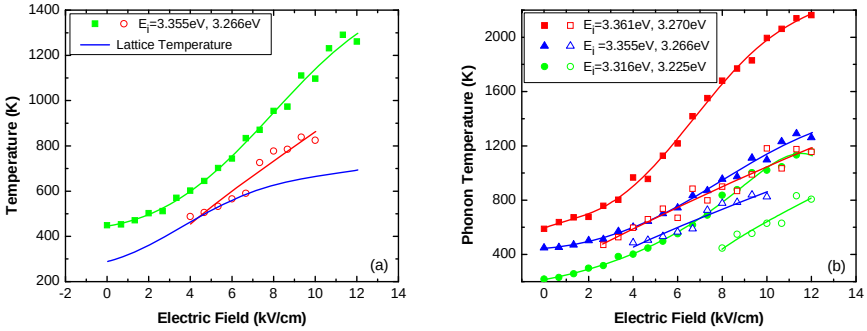

Fig. 2. LO phonon temperature measured by first-order (solid symbols) and second-order (open symbols) Raman scattering and lattice temperature [the lowest curve (blue) in (a)] as a function of applied electric field. Energies of incident photons are given by legends.

This work has been supported by DARPA/AFOSR.

[1] K. T. Tsen, D. K. Ferry, A. Botchkarev, B. Sverdlov, A. Salvador, and H. Morkoç, "Direct measurements of electron-longitudinal optical phonon scattering rates in wurtzite GaN," Appl. Phys. Lett. **71**, 1852-1853 (1997); "Time-resolved Raman studies of the decay of the longitudinal optical phonons in wurtzite GaN," Appl. Phys. Lett. **72**, 2132-2134 (1998).

[2] A. Matulionis, J. Liberis, I. Matulioniene, M. Ramonas, L. F. Eastman, J. R. Shealy, V. Tilak, A. Vertiatchikh, "Hot-phonon temperature and lifetime in a biased $Al_xGa_{1-x}N$/GaN channel estimated from noise analysis," Phys. Rev. B **68**, 035338 (2003).

[3] T. Palacios, A. Chakraborty, S. Heikman, S. Keller, S. P. DenBaars, and U. K. Mishra, "AlGaN/GaN High electron mobility transistors with InGaN back-barriers," IEEE Electron Dev. Lett. **27**, 13-15 (2006).

[4] D. S. Kim and P. Y. Yu, "Hot-electron relaxations and hot phonons in GaAs studied by subpicosecond Raman scattering," Phys. Rev. B **43**, 4158-4169 (1991).

[5] I. Vurgaftman and J. R. Meyer, "Band parameters for nitrogen-containing semiconductors," J. Appl. Phys. **94**, 3675-3696 (2003).